

Substrate-Solvent crosstalk – effects on reaction kinetics and product selectivity in olefin oxidation catalysis

Rita N. Sales,^[a] Sam K. Callear,^[b] Pedro D. Vaz,^{[c,d]*} Carla D. Nunes^{[a]*}

^[a] Centro de Química Estrutural, Faculdade de Ciências da Universidade de Lisboa, 1749-016 Lisboa, Portugal

^[b] ISIS Neutron & Muon Source, Rutherford Appleton Laboratory, Chilton, Didcot, Oxfordshire OX11 0QX, United Kingdom

^[c] CICECO – Aveiro Institute of Materials, Department of Chemistry, University of Aveiro, 3810-193 Aveiro, Portugal

^[d] Champalimaud Foundation, Champalimaud Centre for the Unknown, 1400-038 Lisboa, Portugal

Correspondence to:

Dr. Carla D. Nunes

Centro de Química Estrutural, Departamento de Química e Bioquímica, Faculdade de Ciências da Universidade de Lisboa, Campo Grande, Ed. C8, 1749-016 Lisboa, Portugal

e-mail: cmnunes@ciencias.ulisboa.pt

Tel: (+351) 217 500 876

Fax: (+351) 217 500 088

Dr. Pedro D. Vaz

Champalimaud Foundation, Champalimaud Centre for the Unknown, 1400-038 Lisboa, Portugal

e-mail: pedro.vaz@fundacaochampalimaud.pt

Tel: (+351) 210 480 200

Fax: (+351) 210 480 299

Abstract

In this work we explored how solvents can affect olefin oxidation reactions catalyzed by MCM-bpy-Mo catalysts and whether their control can be made with those players. The results of this study evidenced that polar and apolar aprotic solvents modulated the reactions in different ways. Experimental data showed that acetonitrile (aprotic polar) could hinder largely the reaction rate whereas toluene (aprotic apolar) did not. In both cases product selectivity at isoconversion was not affected. Further insights were obtained by means of neutron diffraction experiments, which confirmed the kinetic data allowing to propose a model based on substrate-solvent crosstalk by means of hydrogen bonding. In addition, the model was also validated in the ring-opening reaction (overoxidation) of styrene oxide towards benzaldehyde, which progressed when toluene was the solvent (reaching 31% styrene oxide conversion) but was strongly hindered when acetonitrile was used instead (reaching only 7% conversion), due to the establishment of H-bonds in the latter.

Although this model was confirmed and validated for olefin oxidation reactions, it can be envisaged that it may also be applied to other catalytic reaction systems where reaction control is critical, while widening its use.

1. Introduction

Developing selective reactions is an everyday struggle that mankind fights to replicate Nature's work, which is remarkable at all levels. Mankind is continuously trying to mimic something that has already millions of years of perfection and therefore the effort is massive to reach it.

In the case of oxidation reactions, the quest for selective processes poses an everyday challenge to both academy and industry [1-7]. To achieve that goal catalysts have been developed to address the need of operating chemical transformations in an efficient and selective way. That has driven much research focusing in the very different and specific oxidation reactions, provided by the plethora of functional groups requiring oxidation, that are needed for assessing added-value products [8-10]. Focusing on obtaining, ideally, a single product, control of the chemical process is critical to achieve this goal, which implies that several parameters need to be known, so that one knows how to control it [4]. In the simplest cases this can be done based on

the kinetics of the reaction. However, this is rare and as such, catalysis is detrimental to progress such quest tuning selectivity sometimes at the cost of activity. This becomes even more pertinent given the sustainability goals that must be met according to commitments by several stakeholders [3,5,7].

Research in catalytic process optimization covers catalyst development ranging from a choice of several transition metals (mostly) and their ability to work under a choice of homogeneous or heterogeneous versions with a wide range of supporting materials available [11-13]. Beyond that, research also devotes effort to find the most suitable oxygen source (ideally dioxygen, but also organic peroxides or hydrogen peroxide), physical conditions (pressure and temperature) and the solvent [14-17]. Solvent choice is usually screened in terms of finding a sweet spot in the activity/selectivity balance, with the ultimate choice being made, eventually, from a sustainability point of view [18,19]. However, little attention has been devoted to assessing what specific phenomena rule the differences observed in a given process when the solvent is changed. For instance, some reports on the catalytic oxidation of styrene showed that authors screened a set of solvents and made their choices depending on the best one to achieve the highest conversion, selectivity or both [20-27]. However, assessment of solvent effects was done on the basis of the nature of the solvent, i.e., protic/aprotic or polar/apolar without going further deep than that [28-31]. Further insights on the local structure and effects of solvents at the molecular level are still scarce and in great need to contribute for the development of more sustainable processes.

Recently, a few reports tried to address the influence of liquid solvents in the activity of several catalytic systems [32-34]. For instance, Emenike described how different solvents can modulate the existence of C–H $\cdots\pi$ interactions between solvents and solutes with implications on the conformational behavior of the latter [32]. In another study using total neutron scattering, authors assessed the structure of a series of aromatic organics with increasing degree of unsaturation at the side chain (ethyl benzene, styrene and phenylacetylene) [35]. In that study, by looking at the solvation shells, authors found that the unsaturation did not have much influence on the existence of intermolecular interactions with a preference for chain-chain vicinity.

In this work we describe solvent effects observed in oxidation catalysis and how they influence both substrate conversion and, in some cases, product selectivity. Specifically, experimental

evidence on how the solvent interferes with the catalytic system is provided. Data is discussed on the feasibility of the proposed model and supported by experimental and computational data.

Experimental procedures

General

All reagents were purchased from Aldrich and used as received.

FTIR spectra were measured with a Nicolet Nexus 6700 FTIR spectrometer using Diffuse Reflectance accessory for clay materials. All FTIR spectra were measured in the 400-4000 cm^{-1} range and using 4 cm^{-1} resolution. Powder XRD measurements were taken on a Philips Analytical PW 3050/60 X'Pert PRO (theta/2 theta) equipped with X'Celerator detector and with automatic data acquisition (X'Pert Data Collector (v2.0b) software), using monochromatized Cu-K α radiation as incident beam, 40 kV–30 mA. Microanalyses were performed at the University of Vigo. The oxidation reactions described in this study were catalyzed by an Mo organometallic complex immobilised inside the pores of MCM-41 by means of a tethered bipyridine ligand. This catalyst, denoted MCM-bpy-Mo, was reported earlier [26,36] and its synthesis is described in the SI material. Furthermore, for the validation of the solvent effects described here, one batch of MCM-41 was also synthesized and then split into two sub-batches differing in the protocol for template removal – one sub-batch was calcined, being denoted MCM_C, while the other was subjected to a template removal procedure by refluxing it with methanol acidified with HCl, being denoted MCM_{AW}. This rendered a set of MCM with regular surface silanol groups (MCM_C), while the remaining (MCM_{AW}) would have Brønsted acid silanol groups. Details of the synthesis procedures can be found in the SI material as well.

All catalytic reactions were conducted in a Carousel 12 Plus Reaction Station from Radleys, providing both temperature and atmosphere control. All reactions were monitored (substrate conversion and product yield) by sampling at regular time intervals and analyzed using a Shimadzu QP-2010 Plus GC-MS system.

General procedure for catalytic epoxidation of olefins

The olefin substrates (1.6 mmol) – *cis*-cyclooctene, styrene, *trans*-2-hexen-1-ol, *R*-(+)-limonene – were mixed with dibutylether (1.6 mmol, internal standard) and 15 μL (5 mol %) of *tert*-butyl

hydroperoxide (5.5 M solution in decane; tbhp) followed by addition of the solvent (acetonitrile or toluene) and MCM-bpy-Mo catalyst.

General procedure for the metal-free oxidation of styrene oxide towards benzaldehyde

The procedure was very similar to the previous one. Styrene oxide (1.6 mmol) was mixed with dibutylether (1.6 mmol) (internal standard) and 15 μ L (5 mol %) of *tert*-butyl hydroperoxide (5.5 M solution in decane; tbhp) followed by addition of the solvent (acetonitrile or toluene). Then the MCM-41 catalyst (either MCM_C or MCM_{AW}, 3 mol%) was added to this mixture. The magnetically stirred mixture was heated to 353 K and kept for 24 h.

Results and Discussion

Solvent Effects on the Catalytic Oxidation of Olefins

Across research on the development of efficient systems for the catalytic oxidation of olefins several physical parameters are usually tuned. However, through the course of past reports, we noticed that the reaction kinetics on substrate conversion would be drastically affected by changing the solvent.

Previous reports found in the literature have described several levels of solvent effects depending on the systems studied. For instance, Zhenyan reported the solvent affected drastically the performance of a catalytic styrene oxidation system [28]. The authors reported the use of polar solvents with the protic ones hindering largely the reaction mostly in terms of substrate conversion.

In this study we addressed how solvents – acetonitrile (polar aprotic) and toluene (apolar aprotic) – interfered in the catalytic oxidation of a set of olefins. This was evidenced for the oxidation of *cis*-cyclooctene, styrene, *R*-(+)-limonene and *trans*-hex-2-en-1-ol, in the presence of MCM-bpy-Mo catalyst and using *tert*-butylhydroperoxide (tbhp) as oxygen source.

As can be seen from Figure 1, data from conversion of the different substrates catalyzed by the above-mentioned system showed that the reaction rates were found to be dramatically dependent on the solvent under strictly similar conditions.

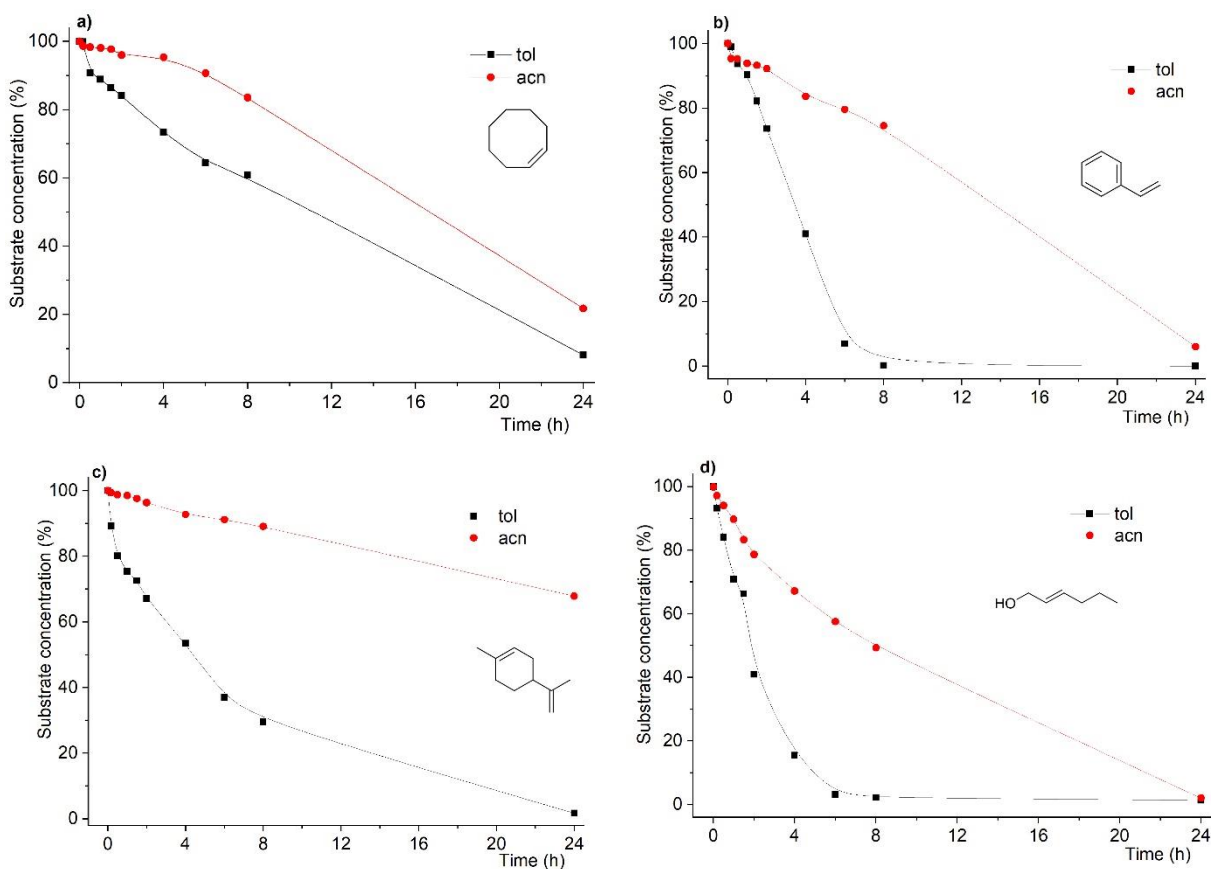


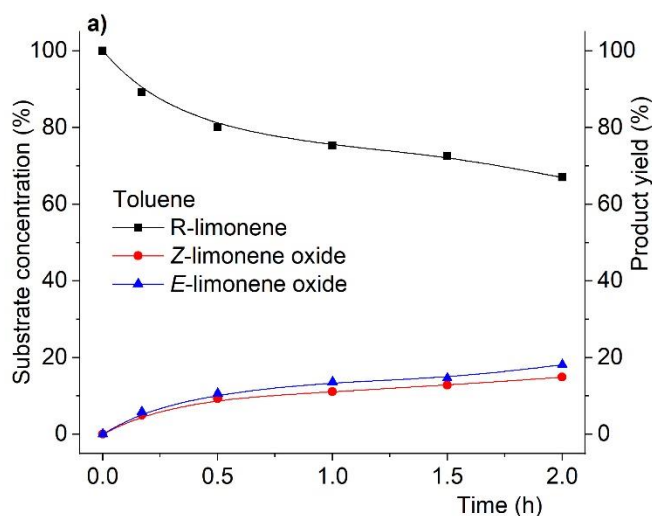
Figure 1. Kinetic profiles of substrate conversion for oxidation reactions of selected olefin substrates in toluene and acetonitrile. It can be clearly seen the dramatic solvent effect experienced by the reaction rate, much lower when acetonitrile is the solvent.

Still, another feature arises from the data in Figure 1. Not only the reaction rates were affected by the solvent change, but also the final conversion after 24 h was found to follow the same dependence. As such, for most of the substrates, when acetonitrile was used as solvent, with the exception of the *trans*-hex-2-en-1-ol substrate, we found that the final conversions were lower, in some case drastically, as in the case of *R*-(+)-limonene.

In the case of styrene, Figure 1b, the main desired product is styrene oxide. However, formation of benzaldehyde is commonly observed and often as major product. This has already been addressed by us, when using MCM-based catalysts, which due to specific surface species are responsible for conversion of styrene into benzaldehyde [26,37]. In the results obtained in this study using the MCM-bpy-Mo catalyst, product yield was found to be dependent on the solvent

used. In fact, when the solvent was toluene, styrene oxidation yielded benzaldehyde with 75% yield (styrene oxide with 25 % yield) at 100% substrate conversion, after 24 h reaction time. On the other hand, when the reaction was conducted in acetonitrile product yield changed a lot: 48% for benzaldehyde and 46% for styrene oxide were obtained at 94% substrate conversion after 24 h reaction time. This will be further addressed later in this study to demonstrate that the right choice of solvent could protect styrene oxide from overoxidation.

Concerning product yield (and inherently their selectivity) in the oxidation of *R*-(+)-limonene, we also found that virtually no changes were observed at isoconversion (i.e., conversion at similar values but obtained at different reaction times), when the solvent changed. This is most evident in Figure 2, showing the reaction profile (substrate conversion and product yield) for *R*-(+)-limonene oxidation. As can be seen, at the same conversion level (ca. 34%) the product yield distribution is completely similar with both solvents. The striking difference, as mentioned before, was that the 34% conversion were obtained after 2 h in toluene, but only after 24 h in acetonitrile.



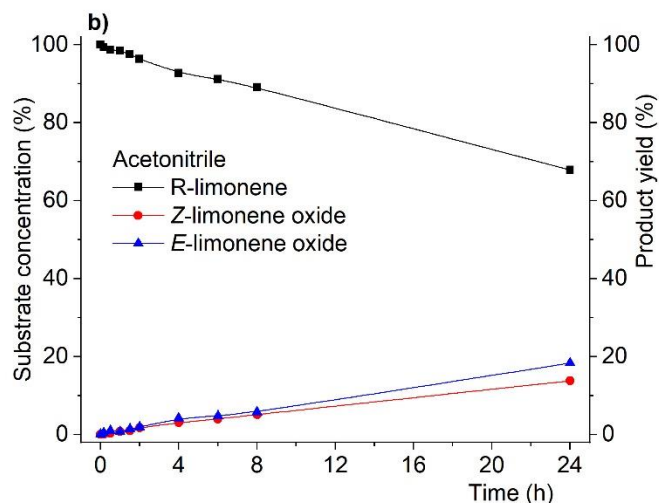


Figure 2. Reaction profiles for *R*-(+)-limonene oxidation catalyzed by MCM-bpy-Mo catalyst in toluene (a) and acetonitrile (b) at substrate isoconversion. It should be noted that substrate isoconversion (33%) was obtained after 2 h (in toluene) and after 24 h (acetonitrile).

As shown in Figure 2, these results showed that changing the solvent did not affect both product yield and product diastereoselectivity ratio at isoconversion. In addition, these data also reveal that the solvent seems to influence solely the reaction kinetics without promoting any apparent deeper interference in the mechanism of the catalytic reaction.

Based on these results it could be likely to assume the possibility for the existence of specific solvent-substrate (or reactant) interactions such as hydrogen bonding, which could be rationalized with acetonitrile but less with toluene [38,39].

Based on recent reports for assessing the structure of liquids by means of neutron scattering techniques [35,40], we have in this work conducted an experiment to assess the local structure of styrene and the solvents mentioned above (acetonitrile and toluene) under the same *in operando* catalysis conditions. Styrene was chosen given that it is readily available as a deuterated isotopomer, which is a requirement for such experiments.

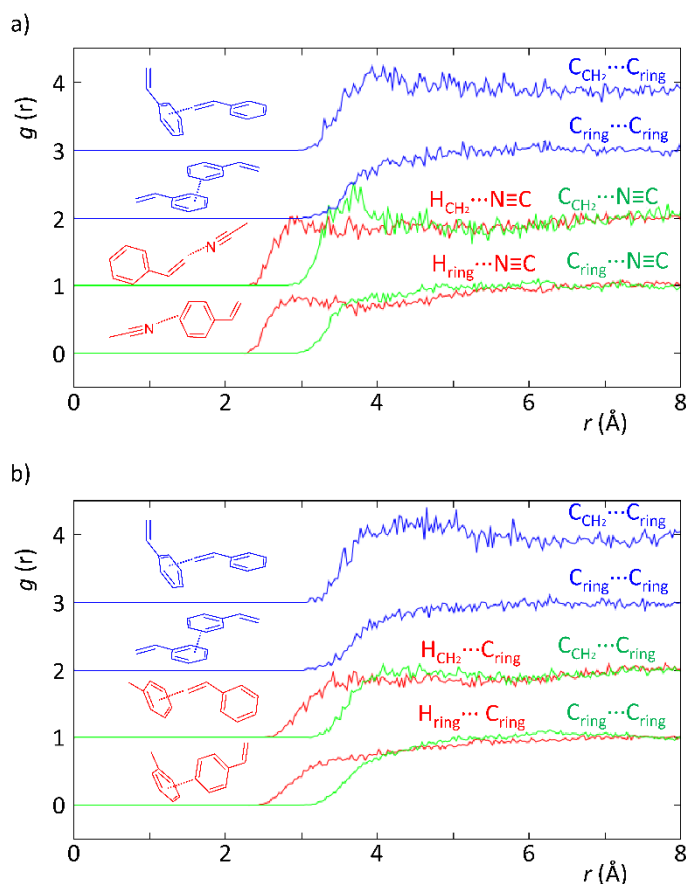


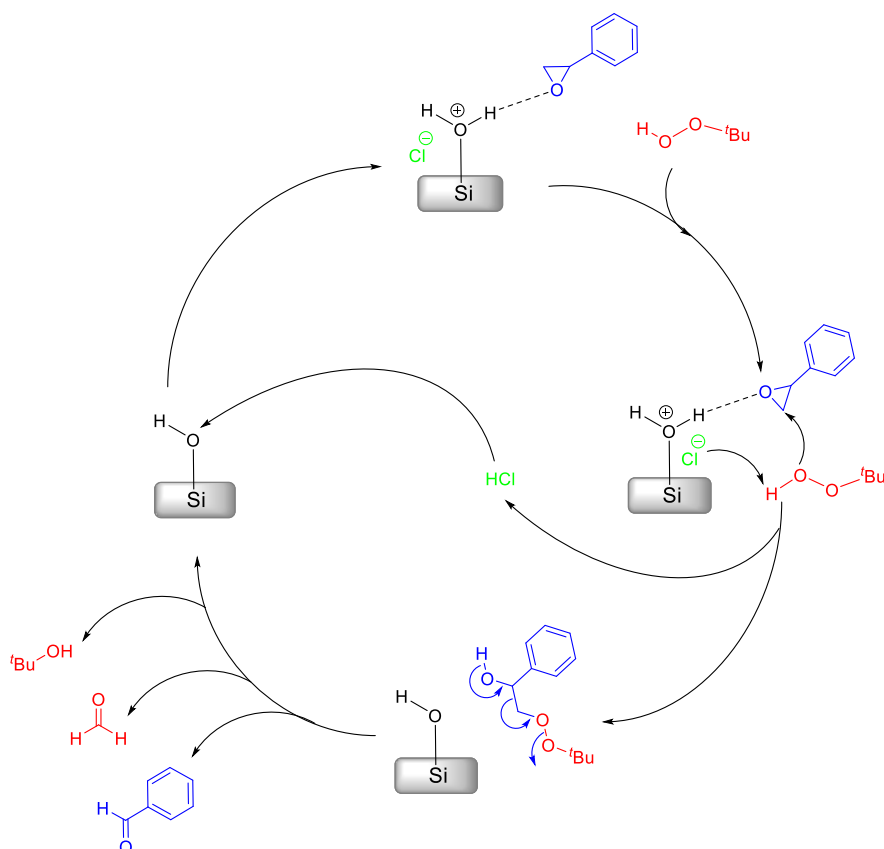
Figure 3. Partial radial distribution functions from EPSR simulation of experimental data obtained with SANDALS data from RB1600022 on the styrene:acetonitrile (a) and styrene:toluene (b) data replicating the ratios used in a catalytic experiment.

According to Figure 3, the neutron diffraction experiment demonstrated that there are differences correlated with the intermolecular interactions between styrene and the solvents (acetonitrile and toluene). In particular, the EPSR model revealed the existence of H-bonds when acetonitrile was present, whereas these were absent when toluene was used instead. This is evidenced in Figure 3a by the $H_{CH_2} \cdots N \equiv C$ and $H_{ring} \cdots N \equiv C$ curves, which show a more defined peak than those in Figure 3b for the curves representing the $H_{CH_2} \cdots C_{ring}$ and $H_{ring} \cdots C_{ring}$ interactions. The reason supporting the fainter peak profile in the latter is indicative of the existence of weaker intermolecular interactions. In fact, this is expected since in the styrene-toluene system (Figure 3b) intermolecular interactions are mostly $C-H \cdots \pi$ whereas in the styrene-acetonitrile system (Figure 3a) the interactions are mostly $C-H \cdots N$, which are stronger yielding therefore a higher degree of organization of the mixture as evidenced. This is verified in Figure 3a, where the

$\text{H}_{\text{CH}_2} \cdots \text{N} \equiv \text{C}$ curve clearly shows the existence of H-bonding between the acetonitrile N-atom and H-atoms in the vinyl group of styrene at lower interaction distances than those found for the H-atoms from the vinyl group and toluene. In addition, the $\text{C}_{\text{CH}_2} \cdots \text{N} \equiv \text{C}$ curve also displays a very defined peak at 3.6-3.8 Å, confirming the existence of specific geometries most probably interacting by means of hydrogen-bonds. These results provide clear and strong evidence that the existence of specific interactions between solvent and substrate are very likely to be responsible for the observed kinetic effects and substrate conversion levels.

Solvent effects in conversion of styrene oxide – model validation

As already mentioned earlier in this study, styrene oxidation is a bit of an issue when it comes to product yield (and subsequently selectivity) in the presence of MCM-41 based catalysts [26,37,41]. In those works, the products were always styrene epoxide and benzaldehyde, the latter being formed either directly or by overoxidation of the former [42], with their relative selectivity presenting different results depending on the used catalyst. We have recently postulated a mechanism that would be responsible for the conversion of styrene oxide into benzaldehyde and formaldehyde [26,37]. That mechanism relies on a side reaction at the MCM surface, rich in silanol groups, without the need of a metal catalyst, being therefore a metal-free process, as evidenced in Scheme I.

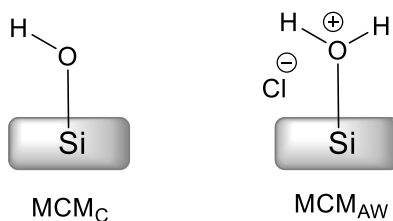


Scheme I

According to Scheme I, styrene oxide binds to a Brønsted acid-site in the first step. Afterwards, the Cl^- abstracts an H-atom from *tbhp*, which will then attack the activated epoxide leading to the opening of the oxirane ring. Concomitantly, this also releases the HCl molecule. The intermediary formed will then decompose yielding benzaldehyde, formaldehyde and *t*-butanol. The previously released HCl molecule binds to the surface silanol regenerating the Brønsted acid-site and closing the cycle.

This proposal lacked confirmation so far. In this way, we used the specific solvent effects concept to test and validate this mechanistic proposal on the conversion of styrene epoxide into benzaldehyde [26,37], while at the same time provided insight about the active role of solvents. To accomplish this, we have used the set of two MCM-41 related materials, MCM_C and MCM_{AW} , differing in the template extraction method (see Experimental Section for details). These MCM materials, as pictured in Scheme II, had their surface with regular silanol groups

(MCM_C) and with Brønsted acid silanol groups (MCM_{AW}) required to assist in the ring-opening process as postulated (Scheme I) [23,35].



Scheme II

As such, starting from styrene epoxide we tested both MCM materials by running the reaction in toluene at 353 K for 24 h (with tbhp) to check whether benzaldehyde could be obtained in the presence of any of the solids (MCM_C and MCM_{AW}). The results evidenced that benzaldehyde could not be obtained in the presence of MCM_C but when using MCM_{AW} the reaction proceeded normally with benzaldehyde being detected, Figure 4.

In the case of the reaction carried out in the presence of MCM_C, styrene oxide conversion was found to be 2% when the solvent was toluene, but when the reaction was conducted in acetonitrile absolutely no reaction was observed (0% styrene oxide conversion).

On the other hand when the catalyst was MCM_{AW} strikingly different results were obtained. According to Figure 4, styrene oxide conversion into benzaldehyde was observed to reach 31% for after 24 h reaction when using toluene as solvent. Changing the solvent to acetonitrile implied a drastic change as only 7% styrene oxide conversion to benzaldehyde compared to the same reaction in toluene.

The first outcome was that this showed that the presence of surface silanol groups with the acid molecules as postulated in Scheme I was needed for the reaction to take place. The second outcome was that we could also demonstrate that the solvent can actively influence the reaction kinetics by establishment of specific intermolecular interactions (e.g., H-bonds) as already discussed earlier in this study and confirmed by neutron diffraction experiments. In fact, the presence of acetonitrile seems to compete with the activated surface silanol groups and thus hinders the reaction. On the other hand, in the case of toluene this effect did not happen to the same extent and competition with silanol groups is not strong enough to hinder the reaction. This concept must be postulated within the framework of the existence of specific intermolecular

interactions – $C-H \cdots N$ and $C-H \cdots \pi$ – as discussed earlier in this study, where their existence will interfere in the reaction rate by interaction with the substrate.

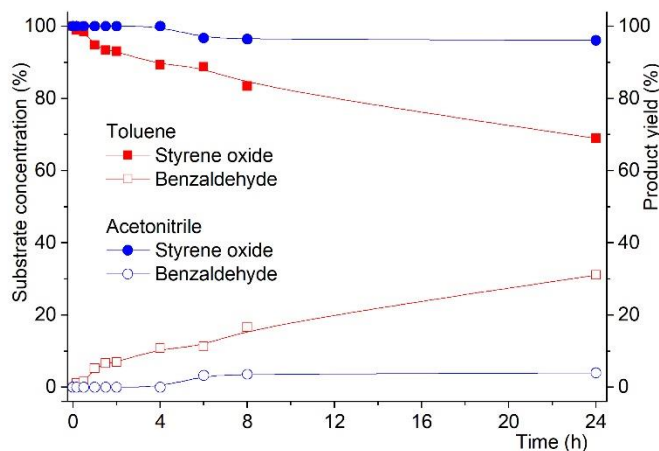


Figure 4. Reaction kinetics for the oxidation of styrene oxide towards benzaldehyde in the presence of MCM_{AW} . The latter is formed when the reaction proceeds in toluene but not in acetonitrile.

The above assumptions were evaluated for feasibility under the framework of DFT calculations to assess possible structures of styrene oxide with solvent molecules. As can be seen in Figure 5, the optimized structures of styrene oxide with solvent molecules (acetonitrile or toluene) evidence the presence of specific interactions through H-bonds. In the case of toluene, the CH_2 group in styrene oxide can interact with toluene through $C-H \cdots \pi$ bonds, whereas in the case of acetonitrile, the interaction takes place by means of $C-H \cdots N$ bonds.

a)

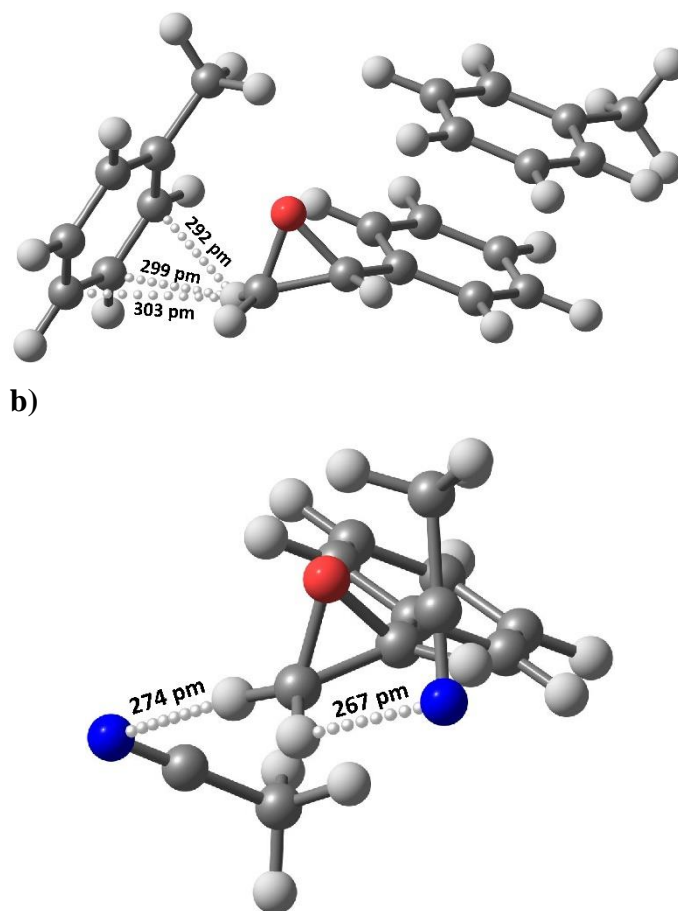


Figure 5. Optimised geometries using a DFT method showing H-bonding interactions between styrene oxide and toluene ($C-H\cdots\pi$; top) or acetonitrile ($C-H\cdots N$; bottom).

DFT results showed that the interaction distance is shorter for the latter – 270 pm on average – compared to that in the former – 298 pm, which render a stronger bonding energy for the $C-H\cdots N$ interactions. These findings were corroborated by NBO topological analyses where the Wiberg bond-orders were 0.009 and 0.002 for the $C-H\cdots N$ and $C-H\cdots\pi$ bonds, respectively. In addition, according to Figure 5a, the represented optimized geometry is showing a free unbonded H-atom in the oxirane ring, which may be also responsible for the reactivity evidenced by this system compared with the geometry found for the acetonitrile version (Figure 5b) where both H-atoms are bonded and unavailable for reaction towards benzaldehyde (Scheme I).

Although the neutron experiments were focused on styrene, these experimental results were obtained for styrene oxide, which is a related substrate. Despite that these data agree with the

results from neutron diffraction discussed earlier in this work for the interactions between styrene and the same solvents, thus validating the model that those solvents play a direct role in the catalytic reaction.

Moreover, the findings from the DFT calculations and those obtained experimentally from the neutron diffraction experiment are coherent and support previous mechanistic proposals that were postulated [26,37]. In our previous mechanistic proposal for the conversion of styrene epoxide towards benzaldehyde it was proposed that the route would occur through an H-bond assisted path. The neutron diffraction data has now shown that in the case of acetonitrile, where much less conversion of styrene epoxide (less benzaldehyde yield) was observed, there are explicit H-bonds. In this way such structure will compete with the H-bond assisted mechanism (Scheme I), resulting in the lower performance of the catalytic system. These data agree with experimental kinetic data as shown above in Figure 4. These findings are in agreement with literature data where intermolecular interactions were described to play a non-innocent role in the structure of liquids, and in styrene in particular [35].

The above results presented and discussed herein demonstrate that for the case of styrene oxidation (and styrene oxide overoxidation) the reaction control can be done by a proper choice of the solvent.

Styrene oxidation leading to the corresponding epoxide or to benzaldehyde (arising from further oxidation of the former) is difficult to control concerning product yield [26-31,37,41] This can be defying when aiming at a specific product, resulting in increased costs and waste due to both the inefficiency of the process and product separation procedures. Recently, there has been evidence for the addition of additives that could prevent further oxidation of reaction products and control its selectivity [43]. This demonstrated how an adequate choice of solvent could modulate product yield, especially in the case when sensitive reaction products were obtained such as styrene oxide.

Conclusions

In this work we have described the differences observed when a given epoxidation reaction is conducted in different solvents. The most striking effect concerns the reaction kinetics, which is largely sensitive to the solvent change. From our research it can be assumed that the hydrogen bond capabilities of a given solvent are relevant enough to support the observed phenomena.

This is true when the solvent was acetonitrile – H-bonding yielding slower kinetics – or toluene – non-H-bonding yielding faster kinetics without major effects on product selectivity at isoconversion for most cases. There was an exception – styrene oxidation – whose both kinetics and product selectivity were found to be affected by the solvent. In this case, it is known that styrene oxide can yield benzaldehyde by over-oxidation. In the present case, we observed that when the H-bonding solvent was used, a much lower amount of benzaldehyde was obtained comparing when the non-H-bonding solvent was used instead. We also extended the concept to confirm a mechanistic proposal on the acid-catalyzed transformation of styrene epoxide into benzaldehyde, which was successfully proved and confirmed the stabilizing effect of an H-bonding solvent in controlling product selectivity.

Summing up, this work provides evidence on the specific role of solvents in contributing to the control of reactions (kinetics and product selectivity) while agreeing with other literature reports under the same scope.

Supplementary Materials: The following are available online: Detailed experimental and computational procedures. Figure S1 – XRD powder patterns of MCM_C and MCM_{AW} materials. Table S1 – Results of catalytic experiments. Coordinates of the optimized geometries for the calculated species represented in Figure 5 and the isolated monomers (styrene oxide, toluene and acetonitrile).

Funding: Fundação para a Ciência e Tecnologia (FCT), Portugal funded this research and is acknowledged for financial support through grants UIDB/00100/2020 and UIDP/00100/2020.

Acknowledgements

Experiments at the ISIS Neutron and Muon Source were supported by a beamtime allocation RB1600022 from the Science and Technology Facilities Council [44]. G09 calculations were made possible due to the computing resources provided by STFC Scientific Computing Department's SCARF cluster.

Author Contributions: R.N.S.: Investigation, Formal Analysis, Writing – Original draft. S.K.C.: Conceptualization, Investigation, Formal Analysis, Data Curation, and Writing – Review and Editing. P.D.V.: Conceptualization, Investigation, Data Curation, Formal Analysis and Writing – Review and Editing. C.D.N.: Conceptualization, Methodology, Supervision, Project Administration, Formal Analysis and Writing – Review and Editing. All authors have read and agreed to the published version of the manuscript.

Data Availability Statement: Data from the neutron scattering experiments can be accessed freely at <https://doi.org/10.5286/ISIS.E.RB1600022>

Conflicts of Interest: All authors declare no conflict of interests.

References

1. Zaccaria, F.; Fagiolari, L.; Macchioni, A. Optimizing noble metals exploitation in water oxidation catalysis by their incorporation in layered double hydroxides. *Inorg. Chim. Acta* **2021**, *516*, 120161. DOI: 10.1016/j.ica.2020.120161
2. Goyal, R.; Singh, O.; Agrawal, A.; Samanta, C.; Sarkar, B. Advantages and limitations of catalytic oxidation with hydrogen peroxide: from bulk chemicals to lab scale process. *Catal. Rev.* **2020**, 1-57. DOI: 10.1080/01614940.2020.1796190
3. Nasrollahzadeh, M.; Sajjadi, M.; Shokouhimehr, M.; Varma, R.S. Recent developments in palladium (nano)catalysts supported on polymers for selective and sustainable oxidation processes. *Coord. Chem. Rev.* **2019**, *397*, 54-75. DOI: 10.1016/j.ccr.2019.06.010
4. Ahn, S.; Hong, M.; Sundararajan, M.; Ess, D.H.; Baik, M.H. Design and Optimization of Catalysts Based on Mechanistic Insights Derived from Quantum Chemical Reaction Modeling. *Chem. Rev.* **2019**, *119*, 6509-6560. DOI: 10.1021/acs.chemrev.9b00073
5. Vedrine, J.C. Metal Oxides in Heterogeneous Oxidation Catalysis: State of the Art and Challenges for a More Sustainable World. *ChemSusChem* **2019**, *12*, 577-588. DOI: 10.1002/cssc.201802248
6. Vedrine, J.C. Heterogeneous Catalysis on Metal Oxides. *Catalysts* **2017**, *7*, 341. DOI: 10.3390/catal7110341
7. Clarke, C.J.; Tu, W.-C.; Levers, O.; Bröhl, A.; Hallett, J.P. Green and Sustainable Solvents in Chemical Processes. *Chem. Rev.* **2018**, *118*, 747-800. DOI: 10.1021/acs.chemrev.7b00571

8. Kajbafvala, A.; Ali, Md.E.; Rahman, Md. M.; Sarkar, S.M.; Hamid, S.B.A. Heterogeneous Metal Catalysts for Oxidation Reactions. *J. Nanomater.* **2014**, 1687-4110. DOI: 10.1155/2014/192038
9. Leus, K. ; Liu, Y.-Y.; Van Der Voort, P. Metal-Organic Frameworks as Selective or Chiral Oxidation Catalysts. *Catal. Rev.* **2014**, *56*, 1-56. DOI: 10.1080/01614940.2014.864145
10. Valange, S.; Vedrine, J.C. General and Prospective Views on Oxidation Reactions in Heterogeneous Catalysis. *Catalysts*, **2018**, *8*, 483; DOI:10.3390/catal8100483
11. Kholdeeva, O.; Maksimchuk, N. Metal-Organic Frameworks in Oxidation Catalysis with Hydrogen Peroxide. *Catalysts* **2021**, *11*, 283. DOI: 10.3390/catal11020283
12. Trehoux, A.; Guillot, R.; Clemancey, M.; Blondin, G.; Latour, J.M.; Mahy, J.P.; Avenier, F. Bioinspired symmetrical and unsymmetrical diiron complexes for selective oxidation catalysis with hydrogen peroxide. *Dalton Trans.* **2020**, *49*, 16657-16661. DOI: 10.1039/d0dt03308a
13. Wang, S.; Liu, Y.; Zhang, Z.; Li, X.; Tian, H.; Yan, T.; Zhang, X.; Liu, S.; Sun, X.; Xu, L.; Luo, F.; Liu, S. One-Step Template-Free Fabrication of Ultrathin Mixed-Valence Polyoxovanadate-Incorporated Metal Organic Framework Nanosheets for Highly Efficient Selective Oxidation Catalysis in Air. *ACS Appl. Mater. Interf.* **2019**, *11*, 12786-12796. DOI: 10.1021/acsami.9b00908
14. Kholdeeva, O.A. Liquid-phase selective oxidation catalysis with metal-organic frameworks. *Catal. Today* **2016**, *278*, 22-29. DOI: 10.1016/j.cattod.2016.06.010
15. Guo, Z.; Liu, B.; Zhang, Q.H.; Deng, W.P.; Wang, Y.; Yang, Y.H. Recent advances in heterogeneous selective oxidation catalysis for sustainable chemistry. *Chem. Soc. Rev.* **2014**, *43*, 3480-3524. DOI: 10.1039/c3cs60282f
16. Boisvert, L.; Goldberg, K.I. Reactions of Late Transition Metal Complexes with Molecular Oxygen. *Acc. Chem. Res.* **2012**, *45*, 899-910. DOI: 10.1021/ar2003072
17. Hermans, I.; Spier, E.S.; Neuenschwander, U.; Turra, N.; Baiker, A. Selective Oxidation Catalysis: Opportunities and Challenges, *Topics Catal.* **2009**, *52*, 1162-1174. DOI: 10.1007/s11244-009-9268-3
18. Fernandes, C.I.; Vaz, P.D.; Nunes, T.G.; Nunes, C.D. Zinc biomimetic catalysts for epoxidation of olefins with H₂O₂. *Appl. Clay Sci.* **2020**, *190*, 105562. DOI: 10.1016/j.clay.2020.105562
19. Fernandes, C.I.; Vaz, P.D.; Nunes, C.D. Selective and Efficient Olefin Epoxidation by Robust Magnetic Mo Nanocatalysts. *Catalysts* **2021**, *11*, 380. DOI: 10.3390/catal11030380
20. Zhang, L.L.; Zhang, Z.Y.; He, X.P.; Zhang, F.; Zhang, Z.B. Regulation of the products of styrene oxidation. *Chem. Eng. Res. Des.* **2017**, *120*, 171-178. DOI: 10.1016/j.cherd.2017.02.012

21. Sun, W.L.; Hu, J.L. Oxidation of styrene to benzaldehyde with hydrogen peroxide in the presence of catalysts obtained by the immobilization of $\text{H}_3\text{PW}_{12}\text{O}_{40}$ on SBA-15 mesoporous material. *React. Kinet. Mech. Catal.* **2016**, *119*, 305-318. DOI: 10.1007/s11144-016-1024-7
22. Fu, Y.H.; Xu, L.; Shen, H.M.; Yang, H.; Zhang, F.M.; Zhu, W.D.; Fan, M.H. Tunable catalytic properties of multi-metal-organic frameworks for aerobic styrene oxidation. *Chem. Eng. J.* **2016**, *299*, 135-141. DOI: 10.1016/j.cej.2016.04.102
23. Neto, A.D.S.; Pinheiro, L.G.; Filho, J.M.; Oliveira, A.C. Studies on styrene selective oxidation over iron-based catalysts: Reaction parameters effects. *Fuel* **2015**, *150*, 305-317. DOI: 10.1016/j.fuel.2015.01.069
24. Wang, Q.; Zhang, Y.; Yu, L.; Yang, H.; Mahmood, M.H.R.; Liu, H.Y. Solvent effects on the catalytic activity of manganese(III) corroles. *J. Porphyr. Phthalocyanines* **2014**, *18*, 316-325. DOI: 10.1142/S1088424614500059
25. Saux, C.; Pierella, L.B. Studies on styrene selective oxidation to benzaldehyde catalyzed by Cr-ZSM-5: Reaction parameters effects and kinetics. *Appl. Catal. A-Gen.* **2011**, *400*, 117-121. DOI: 10.1016/j.apcata.2011.04.021
26. Fernandes, C.I.; Rudić, S.; Vaz P.D.; Nunes, C.D. Looking inside the pores of a MCM-41 based Mo heterogeneous styrene oxidation catalyst: an inelastic neutron scattering study. *Phys. Chem. Chem. Phys.* **2016**, *18*, 17272-17280. DOI: 10.1039/c6cp01243d
27. Bento A.; Sanches, A.; Vaz, P.D.; Nunes, C.D. Catalytic Application of Fe-doped MoO_2 Tremella-Like Nanosheets. *Top. Catal.* **2016**, *59*, 1123-1131. DOI: 10.1007/s11244-016-0631-x
28. Pan, Z.; Hua, L.; Qiao, Y.; Yang, H.; Zhao, X.; Feng, B.; Zhu, W.; Hou, Z. Nanostructured Maghemite-Supported Silver Catalysts for Styrene Epoxidation. *Chin. J. Catal.* **2011**, *32*, 428-435. DOI: 10.1016/S1872-2067(10)60183-0
29. Huang, C.; Zhang, H.; Sun, Z.; Zhao, Y.; Chen, S.; Tao, R.; Liu, Z. Porous Fe_3O_4 nanoparticles: Synthesis and application in catalyzing epoxidation of styrene. *J. Colloid Interf. Sci.* **2011**, *364*, 298-303. DOI: 10.1016/j.jcis.2011.08.066
30. Guin, D.; Baruwati, B.; Manorama, S.V. A simple chemical synthesis of nanocrystalline AFe_2O_4 (A = Fe, Ni, Zn): An efficient catalyst for selective oxidation of styrene. *J. Mol. Catal. A-Chem.* **2005**, *242*, 26-31. DOI: 10.1016/j.molcata.2005.07.021
31. Tong, J.; Cai, X.; Wang, H.; Zhang, Q. Improvement of catalytic activity in selective oxidation of styrene with H_2O_2 over spinel Mg-Cu ferrite hollow spheres in water. *Mater. Res. Bull.* **2014**, *55*, 205-211. DOI: 10.1016/j.materresbull.2014.04.038
32. Emenike, B.U.; Spinelle, R.A.; Rosario, A.; Shinn, D.W.; Yoo, B. Solvent Modulation of Aromatic Substituent Effects in Molecular Balances Controlled by CH- π Interactions. *J. Phys. Chem. A* **2018**, *122*, 909-915. DOI: 10.1021/acs.jpca.7b09910
33. Fraile, J.M.; Garcia, N.; Mayoral, J.A.; Santomauro, F.G.; Guidotti, M. Multifunctional Catalysis Promoted by Solvent Effects: Ti-MCM41 for a One-Pot, Four-Step, Epoxidation-

- Rearrangement-Oxidation-Decarboxylation Reaction Sequence on Stilbenes and Styrenes. *ACS Catal.* **2015**, *5*, 3552-3561 DOI: 10.1021/cs501671a
34. Koohestani, B.; Ahmad, A.L.; Bhatia, S.; Ooi, B.S. *Curr. Nanosci.* **2011**, *7*, 781-789 DOI: 10.2174/157341311797483673
35. Szala-Bilnik, J.; Falkowska, M.; Bowron, D.T.; Hardacre, C.; Youngs, T.G.A. The Structure of Ethylbenzene, Styrene and Phenylacetylene Determined by Total Neutron Scattering. *ChemPhysChem*, **2017**, *18*, 2541-2548. DOI: 10.1002/cphc.201700393
36. Fernandes, C.I.; Saraiva, M.S.; Nunes, T.G.; Vaz, P.D.; Nunes, C.D. Highly enantioselective olefin epoxidation controlled by helical confined environments. *J. Catal.* **2014**, *309*, 21-32. DOI: 10.1016/j.jcat.2013.08.032
37. Zheng, Y.-Z.; Wang, N.-N.; Luo, J.-J.; Zhou, Y.; Yu, Z.-W. Hydrogen-bonding interactions between [BMIM][BF₄] and acetonitrile. *Phys. Chem. Chem. Phys.* **2013**, *15*, 18055-18064. DOI: 10.1039/C3CP53356E
38. Platt, S.P.; Attah, I.K.; El-Shall, M.S.; Hilal, R.; Elroby, S.A.; Aziz, S.G. Unconventional CH^{δ+}...N hydrogen bonding interactions in the stepwise solvation of the naphthalene radical cation by hydrogen cyanide and acetonitrile molecules. *Phys. Chem. Chem. Phys.* **2016**, *18*, 2580-2590. DOI: 10.1039/C5CP06502J
39. Youngs, T.G.A.; Manyar, H.; Bowron, D.T.; Gladden, L.F.; Hardacre, C. Probing chemistry and kinetics of reactions in heterogeneous catalysts. *Chem. Sci.* **2013**, *4*, 3484-3489. DOI: 10.1039/c3sc51477c
40. Silva, N.U.; Fernandes, C.I.; Nunes, T.G.; Saraiva, M.S.; Nunes, C.D.; Vaz, P.D. Performance evaluation of mesoporous host materials in olefin epoxidation using Mo(II) and Mo(VI) active species-Inorganic vs. hybrid matrix. *Appl. Catal. A-Gen.* **2011**, *408*, 105-116. DOI: 10.1016/j.apcata.2011.09.012
41. Fernandes, C.I.; Stenning, G.B.G.; Taylor, J.D.; Nunes, C.D.; Vaz, P.D. Helical Channel Mesoporous Materials with Embedded Magnetic Iron Nanoparticles: Chiral Recognition and Implications in Asymmetric Olefin Epoxidation. *Adv. Synth. Catal.* **2015**, *357*, 3127-3140. DOI: 10.1002/adsc.201500441
42. Nunes, C.D.; Rudić, S.; Vaz, P.D. Probing the Relevance of MoO₂ Nanoparticle Synthesis in Their Catalytic Activity by Inelastic Neutron Scattering. *Phys. Chem. Chem. Phys.* **2020**, *22*, 896-904. DOI: 10.1039/c9cp06278e
43. Sankar, M.; Nowicka, E.; Carter, E.; Murphy, D.M.; Knight, D.W.; Bethell, D.; Hutchings, G.J. The benzaldehyde oxidation paradox explained by the interception of peroxy radical by benzyl alcohol. *Nature Comm.* **2014**, *5*, 3332. DOI: 10.1038/ncomms4332
44. Vaz, P.D., Nunes, C.D., Callear, S. *The active role of solvents in oxidation catalysis*. STFC ISIS Facility, **2015**. DOI: 10.5286/ISIS.E.RB1600022